# Lithospheric Deformation and 3D Mantle Flow in the Pacific-North American Plate Boundary Corner in Southern Alaska

Margarete Jadamec[1]* and Magali I. Billen[1] [1]Department of Geology, University of California, Davis ,CA 95616 USA; *jadamec@geology.ucdavis.edu

**Abstract** The pattern of 3D material flow in a continuum is one proxy used to characterize continental deformation and can yield insights into the physics of convergent margin deformation, specifically the interplay between plate boundary forces, the viscosities of the materials within the tectonic plates, and possibly the importance of plate margin geometry. We use 3D spherical-geometry, finite-element, viscous flow models of the plate boundary system in southern Alaska to test competing hypotheses for the uplift of the central Alaska Range. The spatial correlation of the central Alaska Range with a change in the geometry of the subducted slab implies that features in the subsurface, such as slab shape and/or mantle flow patterns generated therein, may be genetically linked to the uplift of the central Alaska Range. We present here initial results of models from the first phase of our investigations where we examine the influence of slab geometry on the deformation pattern in the overlying lithosphere. The model results suggest that slab geometry is an important factor in determining the distribution of positive and negative dynamic topogrpahy in the overriding lithosphere and that a non-Newtonian rheology may be required to decouple the slab buoyancy from the overriding lithosphere beneath the central Alaska Range.

## Tectonic Setting

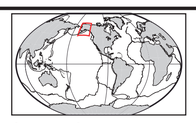

Central Alaska Range
- ~ 500 km inland from plate boundary.
- Actively uplifting since ~ 5-6 Ma.
- Located in magmatic gap.
- Located in region of complex slab shape.

Hypotheses for Uplift of the Alaska Range
- Slab geometry & plate coupling may increase stress transfer inland.
- Varying age, composition, and temperature of accreted terranes cause lateral strength variations in overriding lithosphere.
- Denali Fault System is a weak zone in the overriding lithosphere that localizes uplift.
- Ongoing collision of the Yakutat terrane is required to generate uplift.

In this poster we investigate the first of these hypotheses.

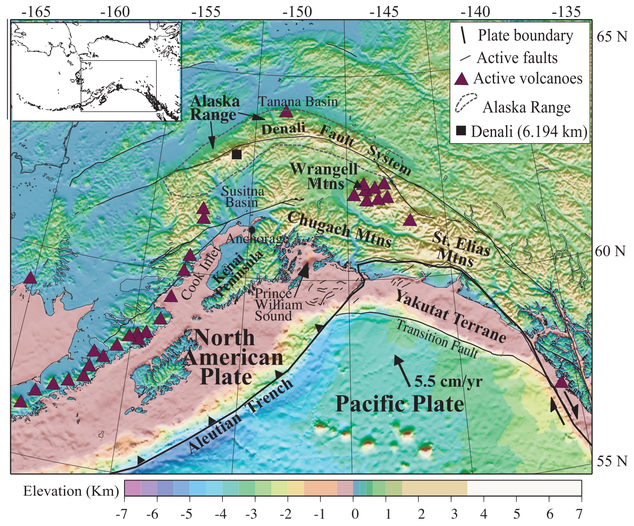


Figure 1. Topography and bathymetry of southern Alaska plate boundary system with major tectonic features superimposed. Note the corner shaped plate boundary which transitions from a northwest trending dextral transform in the east to a northeast trending subduciton zone to the west.

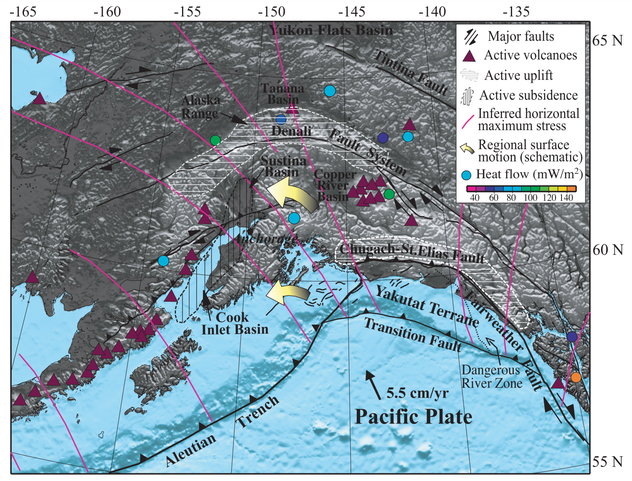


Figure 2. Summary figure of observational constraints on the deformation style of the overriding lithosphere in south-central Alaska. Constraints include: regions of uplift and subsidence, velocity field, stress field, fault slip, and regional heat flow (Plafker et al., 1994; International Heat Flow Commission, 2005; Alaska Volcano Observatory, 2005).

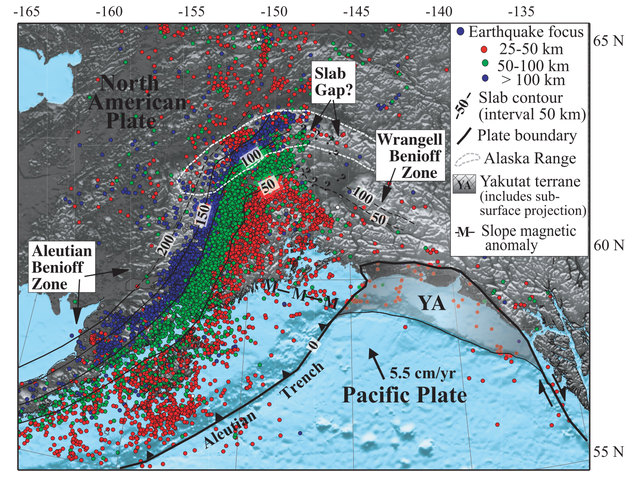


Figure 3. Seismicity (M>3) from 1964-2004 superimposed on topography and bathymetry. Note the bend in Wadati-Benioff zone at -151 W (beneath the west-central Alaska Range and abrupt decrease in seismicity east of ~-147 W). The pattern of seismicity at depth indicates that beneath central Alaska Range the slab orientation changes and that south of the eastern Alaska Range there is either a cusp in the slab and/or a gap below 45 km (Page et al., 1989). Seismic data: Alaska Earthquake Information Center.

## Method

Instantaneous 3D Viscous Flow Finite Element Models, using CitcomT.
- Solves conservation equations of viscous flow for the velocity, **V**, and pressure, p.

Conservation of mass: $\nabla \cdot V = 0$

Conservation of momentum: $\rho g - \nabla p + \nabla \cdot \tau_{ij} = 0$

Formulation of equations are for an incompressible fluid with a high Prandlt number and assume the Boussinesq approximation. ρ is density, t is time, and τ is the viscous stress tensor.

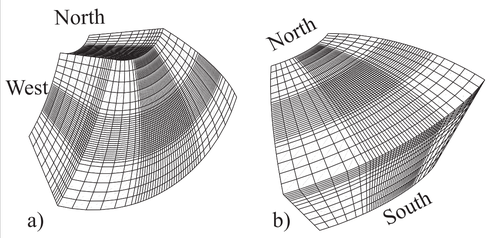


Figure 4. Two perspective views of the 3D multi-resolution mesh used in this study. a) View of the top surface and west and north faces of the model domain. b) View of the top surface and south face of domain. Free slip boundary conditions are applied to each boundary.

- Newtonian rheology (Diffusion creep)

Flow law for olivine

$\dot{\varepsilon} = A\sigma^n d^{-p} C_{OH}^r \exp(-E+PV/RT)$

n=1, p=3, r=1, E=335 kJ,

V= 4 x $10^{-6}$ $m^3$/mol

## Model Input

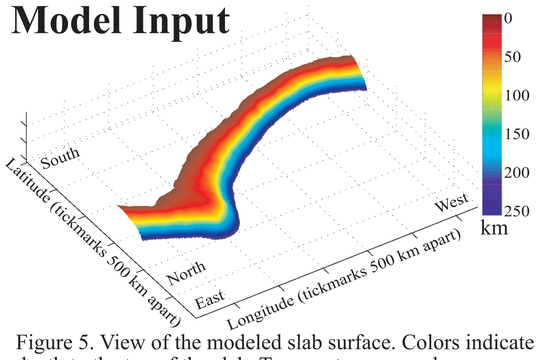


Figure 5. View of the modeled slab surface. Colors indicate depth to the top of the slab. Temperature anomaly was assigned to region between slab surface and the surface extrapolated downward 100 km. Surface was constructed in GMT by interpolating through the following datasets: Ratchkovski and Hansen (2002); Zweck et al. (2002); Gudmundsson and Sambridge (1998); Page et al. (1989).

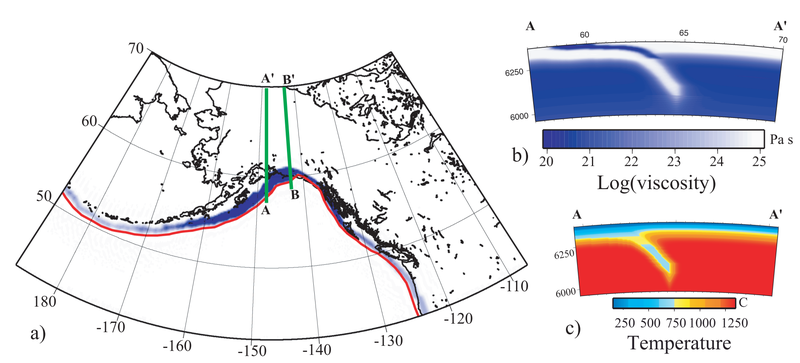


Figure 6. a) Plan view of the viscosity field. A weak region follows the plate interface to a depth of 100 km, both along the trench and along the transform plate boundary. Line AA' marks location of longitudinal slice through (b) viscosity structure and (c) temperature field (this figure). AA' and BB' cross section line locations are also for longitudinal slices in Figure 9. The Juan de Fuca plate is not included in the model.

## Results

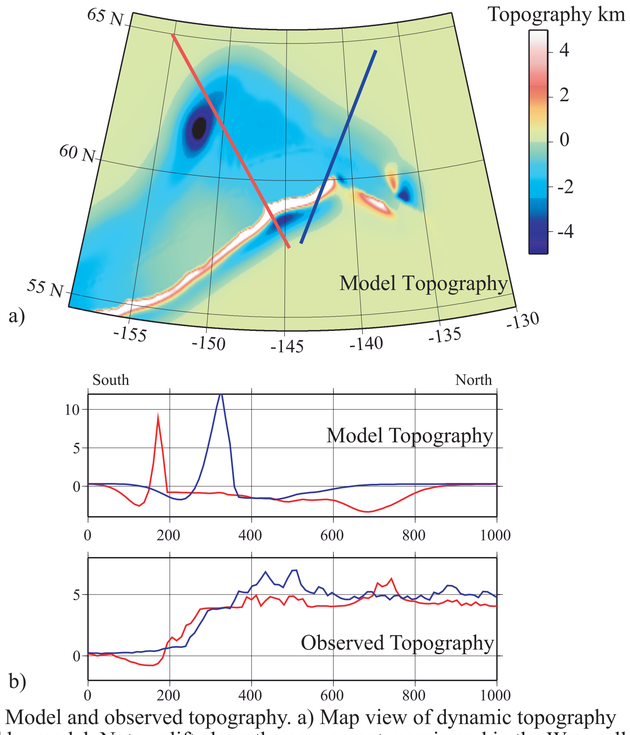


Figure 7. Model and observed topography. a) Map view of dynamic topography predicted by model. Note uplift along the convergent margin and in the Wrangell-St. Elias region. Central Alaska Range coincides with predicted negative dynamic topography (blue bullseye in northwest region of map. Note also topographic low in vicinity of Copper River Basin. b) Cross sections through the Alaska Range (red) and Wrangell Mountains (blue).

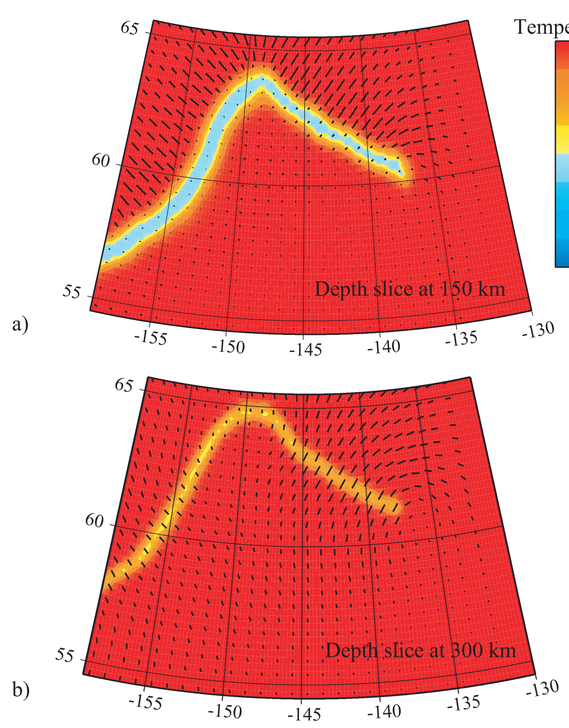


Figure 8. Depth slices of temperature (in color) with superimposed mantle flow pattern (as shown by the relative magnitude of velocity in thick black lines). a) Depth slice is at 150 km. b) Depth slice is at 300 km. Note circular flow pattern around the edge of the slab (model domain side boundaries are > 1000 km away).

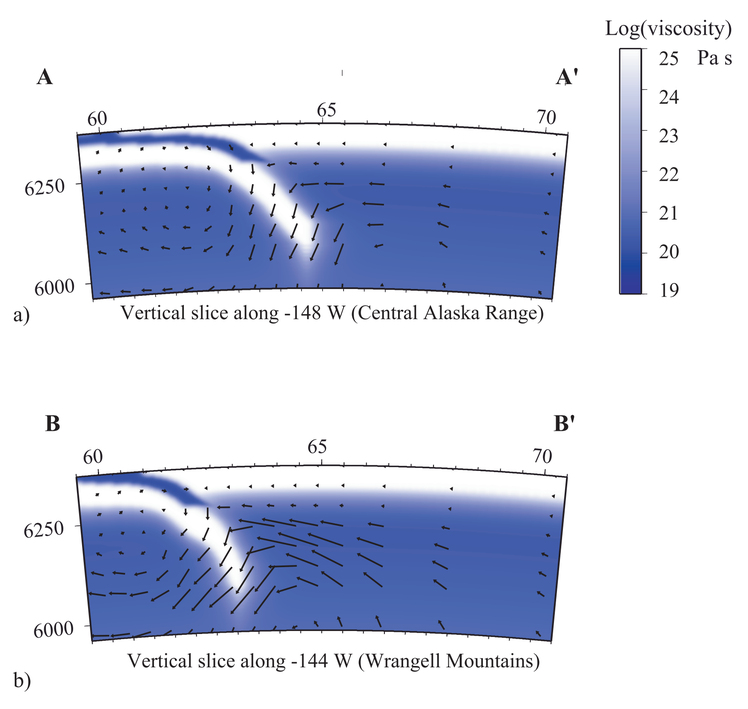


Figure 9. Longitudinal slices of viscosity (in color) with superimposed mantle flow pattern (as shown by the relative magnitude of velocity in thick black arrows). Location of cross sections are shown in Figure 6. Slices are slightly oblique to the slab dip. a) Vertical slice is along -148 longitude. Note the slight downward flow in the mantle wedge. b) Vertical slice is along -144 longitude.

## Discussion

The pattern of predicted dynamic topography indicates that deformation in the overriding lithosphere appears to be concentrated at the plate boundary and where the slab dip steepens beneath the central Alaska Range. Along the plate boundary, in the easternmost plate boundary corner, the model predicts uplift of the St. Elias Mountains (Figures 1, 2 and 7). Although the model does predict positve dynamic topography here and elsewhere along the plate margin, the magnitude of topography is too large and may be reduced in future models by narrowing the weak region along the plate interface. This purely Newtonian model predicts negative dynamic topography in the vicinity of the central Alaska Range, where geologic data indicate there has been recent uplift (Figures 1, 2 and 7). This suggests that the slab buoyancy needs to be decoupled from the overriding lithosphere in order to reduce the negative dynamic topography. Including a non-Newtonian viscosity will weaken the mantle wedge region and decrease the amplitude of the dynamic topography lows. The depth slices of the velocity field indicate a radial pattern of mantle flow around the slab edge (Figure 8). How this pattern compares to that in a model with a slab gap will be assessed in future models. Future models will systematically incorporate a non-Newtonian rheology, a weak zone that represents the Denali Fault System, density and viscosity variations between the Pacific and North American plates, and the Yakutat terrane. Time-dependent models will investigate time varying parameters, such as the collsion of the Yakutat terrane.